Optical investigations of the heavy-fermion superconductor UNi_2Al_3

N. Cao, J. D. Garrett, and T. Timusk
Department of Physics and Astronomy and Institute for Materials Research, McMaster University, Hamilton, Ontario, Canada L8S 4M1

H. L. Liu and D. B. Tanner
Department of Physics, University of Florida, Gainesville, Florida 32611

(Received 6 September 1995)

The optical properties of the heavy-fermion superconductor UNi_2Al_3 have been investigated at temperatures between 10 and 300 K using reflectance spectroscopy. A characteristic energy scale ($\omega_c = 90$ cm^{-1}), with almost the same value as the coherence temperature $T_0 = 100$ K derived from measurements of the dc resistivity and susceptibility, is obtained from the optical conductivity. At high temperatures ($T \geqslant T_0$), this scale represents the energy gap between the ground and excited level that results from the crystal-field splitting of the $5f^2$ ($J=4$) level of the tetravalent uranium ion. In the low-temperature coherent region ($T < T_0$), a narrow, Drude-like, quasiparticle absorption mode develops. This mode is described using a frequency-dependent scattering rate $\Gamma(\omega)$ and mass enhancement factor $\lambda(\omega)$. This free-carrier mode may originate from a hybridization between the $3d$ conduction band of nickel and the $5f$ bands of uranium. Parameters such as the renormalized scattering rate γ^* and plasma frequency ω_P^* of the quasiparticle mode, as well as the quasiparticle bandwidth W at 10 K are derived using the model developed by Millis and Lee.

Heavy-fermion materials, especially those that exhibit the coexistence of antiferromagnetic ordering and superconductivity at low temperatures, e.g., URu_2Si_2 (Ref. 1) and UPt_3 (Ref. 2), have aroused a lot of interest among both experimentalists and theorists. In these materials there is usually a characteristic temperature T_0, above which spin-disorder scattering of the conduction electrons causes the temperature coefficient of the dc resistivity to be negative; below T_0, the scattering is frozen out, resulting in a sharp reduction in resistivity.[3] The temperature dependence of the magnetic susceptibility has a broad peak near T_0 that can be explained by crystal-field splitting.[4] Moreover, susceptibility suggests that the $5f$ moments of the U ions are localized at high temperatures and somehow become delocalized for $T < T_0$. This delocalization has been explained as due to the Kondo effect of the $5f$ spins being compensated by the spins of the conduction electrons.[5] The trouble with this explanation, as noted by Millis and Lee,[6] is that there are not enough conduction electrons within the range of T_K of the Fermi surface, where T_K is the Kondo temperature, to compensate the spins of the ion. Other authors believe that the orbital moment of the ion is so large in these compounds that it results in an almost compensated $5f$ orbital and spin moment.[7] The large electronic specific-heat coefficient γ_e, e.g., $\gamma_e = 422$ mJ/molK^2 for UPt_3,[8] suggests an enhancement of the effective mass of the quasiparticles resulting from the many-body effects of the d conduction electrons and the f electrons of U. Attempts to determine the theoretical ground state which accounts for all these unusual and unique properties of the heavy-fermion materials have been made.[6,9]

Optical reflectance spectroscopy is a very useful technique in the study of these materials because it can probe the electronic excitation spectra of the heavy quasiparticles. The optical properties of the heavy-fermion materials have been studied by reflectance and absorption measurements. Bonn *et al.*[10] measured the temperature dependence of the reflectance of URu_2Si_2 in the far-infrared region, finding a spin-density-wave (SDW) gap at the Fermi surface below T_N and a narrow Drude-like mode developing in the coherent region. A similar mode was found in UPt_3.[11,12] This mode is described within a generalized Drude formula by a frequency-dependent scattering rate and renormalized effective mass.[13]

Recently, two new heavy-fermion superconductors, UNi_2Al_3 and UPd_2Al_3, have been discovered.[14,15] Both undergo antiferromagnetic as well as superconducting phase transition at low temperatures, with $T_N = 4.6$ and 14 K and $T_c = 1$ and 2 K, respectively. The crystal structure of UNi_2Al_3 is of the hexagonal $PrNi_2Al_3$ material (space group $P6/mmm$) with $a = 5.024$ Å and $c = 4.018$ Å and there exists a longitudinal spin density wave with a very small ordered moment $\mu_{\rm ord} \simeq 0.24\mu_B$ in the hexagonal basal plane below T_N.[17] An optical reflectance measurement has been performed on polycrystalline UPd_2Al_3, and a zero-frequency narrow resonance at low temperatures was found.[16]

The single crystal of UNi_2Al_3 used in this measurement was grown at McMaster using the growth process described previously.[17] The crystal quality was characterized using neutron scattering. There are no impurity phases detected. The a-c plane dc resistivity was measured using a four-probe technique. The dc susceptibility was measured by Schroder *et al.*[17] on a second crystal that was used for neutron scattering measurement. Both measurements yield results that are similar to those reported previously.[14] At high temperatures ($T > 150$ K) the resistivity, which is attributed to spin-disorder scattering, saturates, whereas the susceptibility is characteristic of the localized $5f$ electrons of U. A sharp drop in the resistivity below 100 K is accompanied by a broad

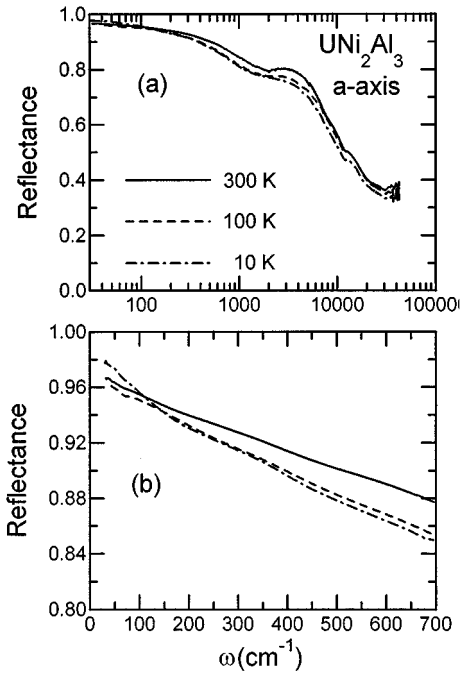

FIG. 1. (a) The polarized reflectance spectra of UNi_2Al_3 along the a axis at 300, 100, and 10 K in the whole measured frequency region. (b) The far-infrared reflectance of UNi_2Al_3 at 300, 100, and 10 K. Note that the magnitude of $R(\omega)$ decreases with decreasing temperature at high frequencies, while the opposite behavior is observed at low frequencies below 100 K. The crossover between the 300 and 10 K data occurs at $\sim 100\ cm^{-1}$, whereas the crossover between 100 and 10 K data occurs at $\sim 150\ cm^{-1}$.

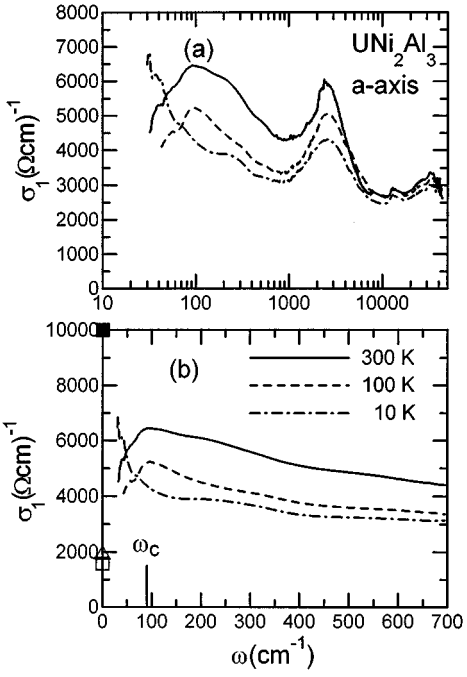

FIG. 2. (a) The real part of the a-axis optical conductivity of UNi_2Al_3 at 300, 100, and 10 K. The conductivity can be fit to a Drude term and four Lorentz oscillators with the fitting parameters being listed in Table I. (b) The far-infrared conductivity of UNi_2Al_3 at 300, 100, and 10 K. The values of the dc conductivity of UNi_2Al_3 at 300 K (square), 100 K (triangle), and 10 K (solid square) as well as a characteristic frequency scale ω_c ($=90\ cm^{-1}$) are indicated. Note that the conductivity declines for frequency below ω_c towards its dc value at 300 and 100 K, whereas a narrow Drude-like peak develops for $\omega < \omega_c$ in the 10 K data.

peak in the susceptibility. This behavior reflects the freezing out of the spin-disorder scattering. Thus, from these two experiments, the characteristic temperature T_0 that separates the spin-disorder from the coherent scattering regions is deduced to be approximately 100 K.

To prepare a UNi_2Al_3 sample suitable for optical measurements, the single crystal was cut parallel to its a-c plane using a spark cutter and was successively polished using the No. 600 diamond grit paper, No. 4000 waterproof silicon carbide paper, 1 μm diamond paste, and finally colloidal alumina solution (0.05 μm Al_2O_3 powder suspended in water). The temperature dependence of the polarized reflectance of the UNi_2Al_3 single crystal has been measured from 30 to 8000 cm^{-1} for temperatures between 10 and 300 K using a Michelson interferometer. The temperature-dependent reflectance between 8000 and 44 000 cm^{-1} was measured at University of Florid using a grating spectrometer. The details of the experimental techniques employed in this work have been described by Homes *et al.*[18] We found that the anisotropy of the reflectance between the a and c axes is very small. The results presented here are for the a axis only.

Figure 1(a) shows the reflectance of UNi_2Al_3 at 300, 100, and 10 K. Generally speaking, the behavior of the reflectance is metallic, decreasing with increasing frequency. The room-temperature reflectance at high frequencies is similar to that of UPd_2Al_3 and has a bump around 3000 cm^{-1} that also appears at low temperatures.[16] The overall reflectance at high frequencies decreases with decreasing temperature from 300 to 100 K and has little temperature dependence between 100 and 10 K. The temperature dependence of the far-infrared reflectance is shown in Fig. 1(b). Its magnitude decreases with decreasing temperature at higher frequencies, but this behavior changes at lower frequencies below 100 K. The crossover occurs at $\sim$ 100 cm^{-1} between the 300 and 10 K data and at $\sim$ 150 cm^{-1} between the 100 and 10 K data. This is typical behavior for the heavy-fermion materials.[10,19] Note the non-Drude behavior of the reflectance at low frequencies for the 300 and 100 K data. This results in the unusual optical conductivity described below.

The real part of the dielectric function $\epsilon_1(\omega)$ and the real part of the optical conductivity $\sigma_1(\omega)$ are obtained from Kramers-Kronig analysis. To perform this transformation one needs to extrapolate the reflectance at both low and high frequencies. The Hagen-Rubens relation is used as an extrapolation to low frequencies. The results in the experimental data region do not depend on a specific low-frequency extrapolation used. Between 40 000 and 10^6 cm^{-1} a power law of ω^{-2} and, beyond this frequency range, a free-electron-like behavior ω^{-4} are used. Figure 2(a) displays the real part of the optical conductivity of UNi_2Al_3 in the whole frequency range at 300, 100, and 10 K. We discuss first the far-infrared conductivity. Figure 2(b) shows the far-infrared conductivity at 300, 100, and 10 K together with the corresponding values for the dc conductivity. It is noted that the extrapolation of the optical conductivity towards zero frequency agrees with the measured dc conductivity. In all

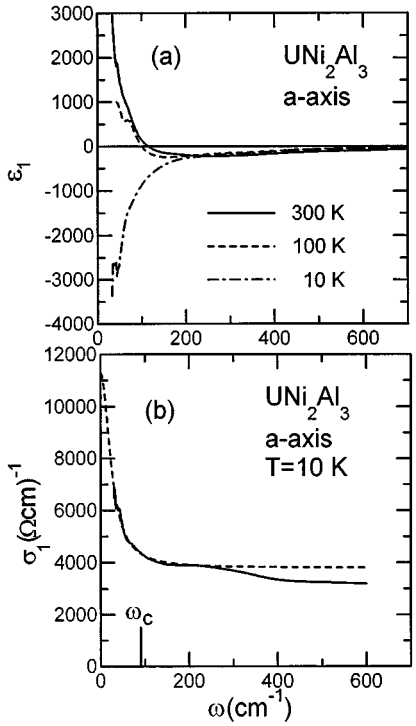

FIG. 3. (a) The real part of the a-axis dielectric function of UNi_2Al_3 at 300, 100, and 10 K. At low frequencies $\epsilon_1(\omega)$ decreases sharply at 10 K due to the narrow Drude-like peak in the 10 K conductivity spectrum, but increases to positive values at 300 and 100 K from the interband transition shown in $\sigma_1(\omega)$ as a peak around ω_c. This transition is due to the crystal-field splitting of the tetravalent $5f^2$ ($J=4$) level of uranium. (b) The solid line is the experimental optical conductivity data of UNi_2Al_3 at 10 K. The dashed line results from a fit up to 200 cm^{-1} using the frequency-dependent term $\sigma_i(\omega)$, as shown in Eq. (1), together with a frequency-independent term σ_m.

three spectra, there exists a characteristic frequency $\omega_c \simeq 90$ cm^{-1} which divides the conductivity spectrum into two different regions. For $\omega > \omega_c$ the conductivity increases with decreasing frequency, as is typical for metals, and its magnitude is reduced as the temperature is lowered. Below ω_c the conductivity begins to decline to the dc conductivity value for the 300 and 100 K data, but rises very rapidly to the dc value at 10 K. Note that the characteristic frequency and the characteristic temperature T_0, deduced from the dc resistivity and susceptibility, are comparable energies.

To see the far-infrared optical behavior more clearly the real part of the frequency-dependent dielectric function $\epsilon_1(\omega)$ of UNi_2Al_3 is shown in Fig. 3(a). At high frequencies $\epsilon_1(\omega)$ is negative at all temperatures. Below ~ 100 cm^{-1} the dielectric function rises dramatically to positive values for the 300 and 100 K curves, but drops sharply at the same frequency at 10 K. We attribute the positive low-frequency $\epsilon_1(\omega)$ at high temperatures to an interband transition. Recently, Steglich *et al.*[20] fit the specific heat to a model that includes a single-site Kondo effect ($S=1/2$, $T_K=48$ K) and a crystal-field splitting of 125 K (~ 90 cm^{-1}) between the doublet of the ground state and the singlet of the first excited state. Also, a gap of ~ 81 cm^{-1}, which is attributed to the crystal-field splitting, shows up in the tunneling spectrum for $T < T_N$.[21] The value of this crystal-field gap coincides with the peak of the conductivity at 300 and 100 K, as shown in Fig. 2(b). The large negative values of $\epsilon_1(\omega)$ in the low-frequency region at 10 K is in accordance with the narrow Drude-like mode shown in the 10 K conductivity spectrum.

Millis and Lee have proposed a theoretical model based on the low-temperature Anderson-lattice Hamiltonian to explain the frequency- and temperature-dependent conductivity.[6] In this model the total conductivity consists of two components, one describing the impurity scattering and the other describing boson fluctuations. The conductivity for the impurity scattering part is

$$\sigma_i(\omega) = \frac{(\omega_P^*)^2 \gamma^*}{4\pi[\omega^2 + (\gamma^*)^2]}, \tag{1}$$

where the renormalized scattering rate $\gamma^* = (m_b/m^*)\Gamma$ (m_b, m^*, and Γ are the band mass, the renormalized mass, and the static scattering rate of the conduction electrons, respectively) and the renormalized plasma frequency $(\omega_P^*)^2 = 4\pi n_e e^2/m^*$ (n_e is the total free carrier density). In this model there is a characteristic frequency ω_c ($\omega_c = 90$ cm^{-1} for UNi_2Al_3) above which $\sigma_i(\omega)$ dies away, causing the conductivity to become independent of frequency at a value of σ_m. This saturation conductivity σ_m is equal to $n_e e^2/(m_b W)$ where W is the quasiparticle bandwidth. Figure 3(b) shows the fit to the 10 K far-infrared conductivity using the formula $\sigma(\omega) = \sigma_i(\omega) + \sigma_m$ [here, we fit $\sigma(\omega)$ up to 200 cm^{-1}]. The parameters obtained from this fit are $\omega_P^* = 3400$ cm^{-1} (~ 0.42 eV), $\gamma_i^* = 25$ cm^{-1} (~ 3.1 meV), and $\sigma_m = 3800$ Ω^{-1} cm^{-1}. The dc conductivity, deduced from the parameters of ω_P^*, γ_i^*, and σ_m, is 11 300 Ω^{-1} cm^{-1} roughly consistent with the measured value of 10 000 Ω^{-1} cm^{-1}. As a check on these parameters, one can estimate the value of ω_P^* from the superconducting properties using the London-penetration-depth formula in the impure limit ($\xi << \lambda_L$),[22]

$$\lambda_P = \lambda_L \left(\frac{\xi}{l}\right)^{1/2} = \frac{c}{\omega_P^*}\left(\frac{\xi}{l}\right)^{1/2}, \tag{2}$$

where ξ and l are the coherence length and the mean free path, respectively. Using the measured values of $l = 470$ Å, $\xi = 240$ Å, and $\lambda_P = 3300$ Å for UNi_2Al_3,[20] one obtains $\omega_P^* = 3400$ cm^{-1}, in fair agreement with the value that we have obtained in this work.

The development of the narrow Drude-like mode seen in the 10 K data is quite common among the heavy-fermion materials in the coherent region (the region where the spin-disorder scattering is frozen out).[11,10,19] It is known that the anomalous properties of the heavy-fermion materials are determined by the behavior of the quasiparticles that result from the hybridization between the d conduction electrons and the localized f electrons of U as the temperature is reduced into the coherent region.[23] The Drude-like mode is governed by the behavior of the quasiparticles, i.e., a large mass and a dramatically reduced scattering at the Fermi level. In studying the optical properties of CrSb, MnSb, NiSb, and NiAs, Allen and Mikkelsen used a generalized Drude formula to get the frequency-dependent scattering rate $\Gamma(\omega)$ and renormalization factor $\lambda(\omega)$ of these materials.

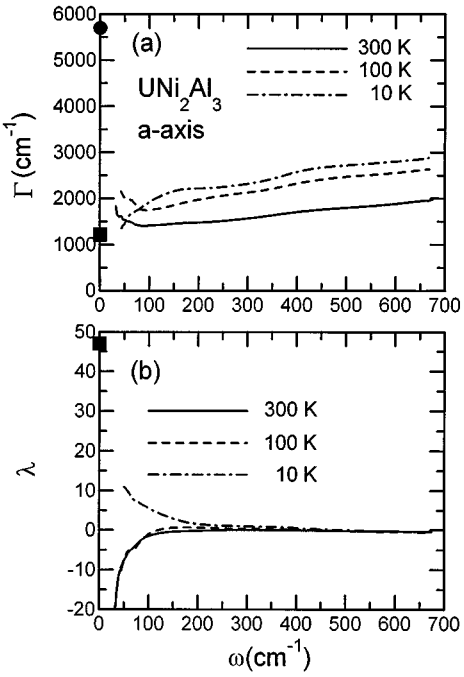

FIG. 4. (a) The frequency-dependent scattering rate of UNi_2Al_3 at 300, 100, and 10 K. The values of $\Gamma(0)$ at 300 and 10 K are represented by the solid circle and square on the left vertical axis, respectively. (b) The frequency-dependent renormalization factor of UNi_2Al_3 at 300, 100, and 10 K. The value of $\lambda(0)$ at 10 K is given by the solid square on the left vertical axis.

The mass enhancement $m^*/m_b=1+\lambda(\omega)$.[13] The same scheme was used in analyzing the conductivity data of UPt_3, URu_2Si_2, and UNi_2Si_2 materials as well as the mixed-valence compound $CePd_3$.[11,10,19,24] Here, we use the same formalism to get $\Gamma(\omega)$ and $\lambda(\omega)$ for UNi_2Al_3. To calculate the absolute values of both quantities one must first determine the value of the bare plasma frequency, ω_P. We estimate $\omega_P \simeq 23\,400\ \mathrm{cm}^{-1}$ (~ 2.9 eV) using the static value of $m^*/m_e(=48)$ (Ref. 20) and the relation $\omega_P/\omega_P^*(10\ \mathrm{K})=(m^*/m_e)^{1/2}$ assuming that the band mass $m_b \simeq m_e$ and the free carrier density n_e does not change with temperature. Using the relation $\omega_P^2=4\pi n_e e^2/m_e$, a free carrier density of $n_e=6.1\times 10^{21}\ \mathrm{cm}^{-3}$ is obtained for UNi_2Al_3. This value is less than $n_e=1.09\times^{22}\ \mathrm{cm}^{-3}$ obtained for UPd_2Al_3.[16]

Figures 4(a) and 4(b) show, respectively, the frequency-dependent scattering rate $\Gamma(\omega)$ and renormalization factor $\lambda(\omega)$ of UNi_2Al_3 at 300, 100, and 10 K. We use the fitting parameter $\gamma^*(10\ \mathrm{K})$ obtained previously and the static value $m^*/m_e(=48)$ obtained from the specific heat measurement by Steglich *et al.*[20] to get $\Gamma(0)=[1+\lambda(0)]\gamma^*(10\ \mathrm{K})=1200\ \mathrm{cm}^{-1}$ at 10 K. The values of $\Gamma(0)$ and $\lambda(0)$ are indicated in the figures as solid squares. The value of $\Gamma(0)$ at 300 K, roughly estimated as $\sim 5700\ \mathrm{cm}^{-1}$, is also shown in Fig. 4(a) as the solid circle using the values of the plasma frequency ($\omega_P=23\,400\ \mathrm{cm}^{-1}$) and the dc conductivity (1600 $\Omega^{-1}\ \mathrm{cm}^{-1}$). The scattering rate gently decreases with decreasing frequency and the magnitude increases as the temperature is reduced at high frequencies. Interestingly, $\Gamma(\omega)$ turns up near 100 cm^{-1} towards the high dc value due to the interband transition in the 300 and 100 K data. In contrast, at 10 K, $\Gamma(\omega)$ drops sharply below 150 cm^{-1} towards its dc value. Such a drop has been seen in other heavy-fermion materials.[11,10,19] The renormalization factor $\lambda(\omega)$ drops off below 100 cm^{-1} and becomes negative at lower frequencies. This unphysical result is due to the interband transition at 300 and 100 K. In contrast, $\lambda(\omega)$ turns up to its high dc value at 10 K.

The static scattering rate of UNi_2Al_3 for $T \geqslant T_0$ is quite large due to the spin-disorder scattering of the conduction electrons. $\Gamma(\omega)$ dramatically declines with increasing frequency until $\omega \sim \omega_c$, after which it slightly increases with frequency. For $T<T_0$, $\Gamma(\omega)$ increases with frequency to its saturated value near ω_c. The narrowing of the Drude-like mode found in the 10 K data is due to a small value of $\Gamma(\omega)$ and a further reduction by a factor $[1+\lambda(\omega)]^{-1}$.

The quasiparticle bandwidth W is $\sim 2400\ \mathrm{cm}^{-1}$ (~ 0.30 eV) deduced from the relation $\sigma_m=n_e e^2/(m_e W)$. Using the relation $m_e/m^* \sim T_K/W$,[6] where T_K is the Kondo temperature, we get $T_K \sim 72$ K in comparison with $T_K=48$ K from the fit to the specific heat result.[20] As Lee *et al.* pointed out,[23] the quasiparticle band results from the f bands being moved up to the fermion level and, then, being narrowed by the hybridization with the d conduction band.

We now discuss the high-frequency conductivity. As shown in Fig. 2(a), the overall conductivity at high frequencies decreases with decreasing temperature. We fit the conductivity spectra at 300, 100, and 10 K to a Drude term and four Lorentz oscillators. The parameters of the Drude term at 300 and 10 K have been given above, and for the 100 K case, we assume that the plasma frequency is the same as the one at 300 K and determine the scattering rate using the values of the dc conductivity ($\sim 2000\ \Omega^{-1}\ \mathrm{cm}^{-1}$) and the plasma frequency. The fitting results are listed in Table I. The lowest-frequency Lorentz mode corresponds to the interband transition between the ground and the first excited level that is due to the crystal-field splitting mentioned before. Interestingly, we find that this mode still exists at 10 K with the position shifting to a slightly lower frequency though the narrow Drude-like coherent mode is the dominant one in far infrared at this temperature. Three absorption peaks appear in the high-frequency region at all temperatures: One is around 2700 cm^{-1} while the other two are above 10 000 cm^{-1}. All are attributed to interband transitions. Similar high-frequency absorption peaks have been also found in UPd_2Al_3.[16]

In conclusion, we have investigated the temperature dependence of the optical constants of UNi_2Al_3 using reflectance spectroscopy. A characteristic frequency scale ω_c ($\simeq 90\ \mathrm{cm}^{-1}$), which is comparable to the characteristic temperature T_0 ($\simeq 100$ K) deduced from dc resistivity and susceptibility measurements, is found in the optical conductivity spectra. At high temperatures ($T \geqslant T_0$) this scale represents the peak position of the interband transition due to the crystal-field splitting of the tetravalent $5f^2$ ($J=4$) level of uranium. A narrow Drude-like quasiparticle absorption mode develops below ω_c at low temperatures on account of the hybridization between the $3d$ conduction band of nickel and the $5f$ bands of uranium. Using the Millis-Lee model,[6] we are able to obtain the renormalized scattering rate $\gamma^*=25$

TABLE I. The parameters used to fit the polarized optical conductivity $\sigma_1(\omega)$ of UNi_2Al_3 along the a axis at 300, 100, and 10 K. γ_D and ω_P^D are the scattering rate and plasma frequency of the Drude part and ω_i, γ_i, and ω_P^i are the center position, width, and strength of the ith Lorentz oscillator. All units are in cm^{-1}.

Mode	T (K)		
	300	100	10
γ_D	5700	4550	25.30
ω_P^D	23 370	23 370	3373
ω_1	124.8	106.6	94.43
γ_1	750.5	444.3	797.4
ω_P^1	14 150	8735	13 422
ω_2	2636	2842	2672
γ_2	3320	4649	5270
ω_P^2	28 260	29 983	34 745
ω_3	13 520	13 613	13 468
γ_3	23 220	22 547	19 494
ω_P^3	49 670	47 415	40 565
ω_4	36 390	38 570	38 637
γ_4	42 380	50 585	57 106
ω_P^4	80 980	87 428	92 839

cm^{-1} and the renormalized plasma frequency $\omega_P^*=3400$ cm^{-1} for this narrow mode at 10 K. The quasiparticle bandwidth is also estimated to be ~ 0.30 eV.

We would like to acknowledge B. D. Gaulin for valuable discussions and R. A. Duncan and G. Hewitson for technical support. Work at McMaster was funded by the Natural Science and Engineering Research Council of Canada (NSERC). Work at UF was supported by the National Science Foundation through Grant No. DMR9401676.

[1] T. T. M. Palstra, A. A. Menovsky, J. van den Berg, A. J. Dirkmaat, P. H. Kes, G. J. Nieuwenhuys, and J. A. Mydosh, Phys. Rev. Lett. **55**, 2727 (1985).
[2] G. Aeppli, E. Bucher, C. Broholm, J. K. Kjems, J. Baumann, and J. Hufnagl, Phys. Rev. Lett. **60**, 615 (1988).
[3] M. B. Maple, J. W. Chen, Y. Dalichaouch, T. Kohara, C. Rossel, M. S. Torikachachvili, M. W. McElfresh, and J. D. Thompson, Phys. Rev. Lett. **56**, 185 (1985).
[4] P. Santini and G. Amoretti, Phys. Rev. Lett. **73**, 1027 (1994).
[5] A. Edelstein, Phys. Lett. **27A**, 614 (1968); S. Doniach, Physica **91B**, 231 (1977).
[6] A. J. Millis and P. A. Lee, Phys. Rev. B **35**, 3394 (1987).
[7] M. S. S. Brooks and P. J. Kelly, Phys. Rev. Lett. **51**, 1708 (1983); J. Sticht and J. Kubler, Solid State Commun. **54**, 389 (1985).
[8] A. de Visser, J. J. M. Franse, A. Menovsky, and T. T. M. Palstra, Physica B+C **127B**, 442 (1984).
[9] Piers Coleman, Phys. Rev. Lett. **59**, 1026 (1987).
[10] D. A. Bonn, J. D. Garrett, and T. Timusk, Phys. Rev. Lett. **61**, 1305 (1988).
[11] P. E. Sulewski, A. J. Sievers, M. B. Maple, M. S. Torikachvili, J. L. Smith, and Z. Fisk, Phys. Rev. B **38**, 5338 (1988).
[12] F. Marabelli, G. Travaglini, P. Wachter, and J. J. M. Franse, Solid State Commun. **59**, 381 (1986).
[13] J. W. Allen and J. C. Mikkelsen, Phys. Rev. B **15**, 2952 (1977).
[14] C. Geibel, S. Thies, D. Kaczorowski, A. Mehner, A. Grauel, B. Seidel, U. Ahlheim, R. Helfrich, K. Petersen, C. D. Bredl, and F. Steglich, Z. Phys. B **83**, 305 (1991).
[15] C. Geibel, C. Schank, S. Thies, H. Kitazawa, C. D. Bredl, A. Bohm, M. Rau, A. Grauel, R. Caspary, R. Helfrich, U. Ahlheim, G. Weber, and F. Steglich, Z. Phys. B **84**, 1 (1991).
[16] L. Degiorgi, M. Dressel, G. Gruner, P. Wachter, N. Sato, T. Komatsubara, and Y. Uemura, Europhys. Lett. **25**, 311 (1994).
[17] A. Schroder, J. G. Lussier, B. D. Gaulin, J. D. Garrett, W. J. L. Buyers, L. Rebelsky, and S. M. Shapiro, Phys. Rev. Lett. **72**, 136 (1994).
[18] C. C. Homes, T. Timusk, M. Reedyk, and D. A. Crandles, Appl. Opt. **32**, 2976 (1993).
[19] N. Cao, J. D. Garrett, and T. Timusk, Physica B **191**, 263 (1993).
[20] F. Steglich, U. Ahlheim, A. Bohm, C. D. Bredl, R. Caspary, C. Geibel, A. Grauel, R. Helfrich, R. Kohler, M. Lang, A. Mehner, R. Modler, C. Schank, C. Wassilew, G. Weber, W. Assmus, N. Sato, and T. Komatsubara, Physica C **185-189**, 379 (1991).
[21] J. Aarts, A. P. Volodin, A. A. Menovsky, G. J. Nieuwenhuys, and J. A. Mydosh, Europhys. Lett. **26**, 203 (1994).
[22] T. Van Duzer and C. W. Turner, *Principles of Superconductive Devices and Circuits* (Elsevier, New York, 1981), p. 123.
[23] P. A. Lee, T. M. Rice, J. W. Serene, L. J. Sham, and J. W. Wilkins, Comments Condens. Matter Phys. **128**, 99 (1986).
[24] B. C. Webb, A. J. Sievers, and T. Mihalisin, Phys. Rev. Lett. **57**, 1951 (1986).